original research

Canadian Undergraduate Physics Journal

Journal Canadien des Étudiants en Physique

VOLUME III ISSUE 3 APRIL 2005

Characterization of quantum dot behaviour in live mammalian cells

Ajit Thakur[1], Cécile Fradin[2]

[1]Department of Biology, McMaster University (ajit.thakur@learnlink.mcmaster.ca)
[2]Department of Physics and Astronomy, McMaster University (fradin@physics.mcmaster.ca)

Received 1 February 2005; Accepted 11 February 2005

Abstract

Quantum dots are semiconductor nanocrystals with exceptional optical properties. To assess their usefulness as fluorescent probes in living systems, we studied the reaction of culture cells to the presence of different types of quantum dots. The quantum dots were characterized in solution using fluorescence correlation spectroscopy and then loaded into mammalian cells and imaged using time-lapse video microscopy. While the cells seemed unperturbed by the presence of single quantum dots, they clearly identified large quantum dot aggregates as foreign bodies. Our results highlight the importance of preventing quantum dot aggregation by using a proper hydrophilic layer.

Introduction

Fluorescence is the capacity of some molecules called fluorophores to absorb photons of a certain wavelength and then to re-emit photons at a different wavelength. Fluorescence is an important tool for imaging, allowing fluorophore-tagged molecules to be tracked.

Currently, the dynamics of biological systems are probed primarily using organic fluorophores, which have inherent limitations usually associated with narrow excitation spectra, broad emission spectra, a limited range of colours and a susceptibility to biodegradation. They are also very sensitive to photobleaching, a light-induced inactivation of the fluorophores, which constrains experimental design and data collection procedures. We explored the use of quantum dots (QDs) as a viable alternative to probe live mammalian cells.

The development of QDs as inorganic fluorophores promises to circumvent many of the limitations associated with organic fluorophores[1]. Quantum dots are small (1–10 nm) semiconductor nanocrystals, usually constructed with a CdSe/ZnS core/shell structure[2] (see Figure 1). Quantum dots have very high quantum yields, broad excitation spectra and narrow size-dependent emission spectra that make them perfect for use in single-molecule detection experiments.

Quantum dots are used in experiments where multiple fluorophores need to be detected simultaneously, since a single light source can be used to excite different QDs, whose different emissions are easily separated using standard filter sets. Moreover, QDs display long fluorescence lifetimes and a tendency to blink – two traits that could be useful for the specific identification of single QDs in biological specimens.

In chemical terms, QDs are superior to organic fluorophores due to their customizable size and surface chemistry, allowing multiple molecules to be bound to a single QD. Furthermore, the inorganic composition of QDs makes them resistant to photobleaching and prevents biodegradation in cells. These properties permit their use as long-term probes in live cells. Overall, QDs have outstanding optical, chemical and physical properties that make them ideal candidates for the investigation of live cell dynamics[1].

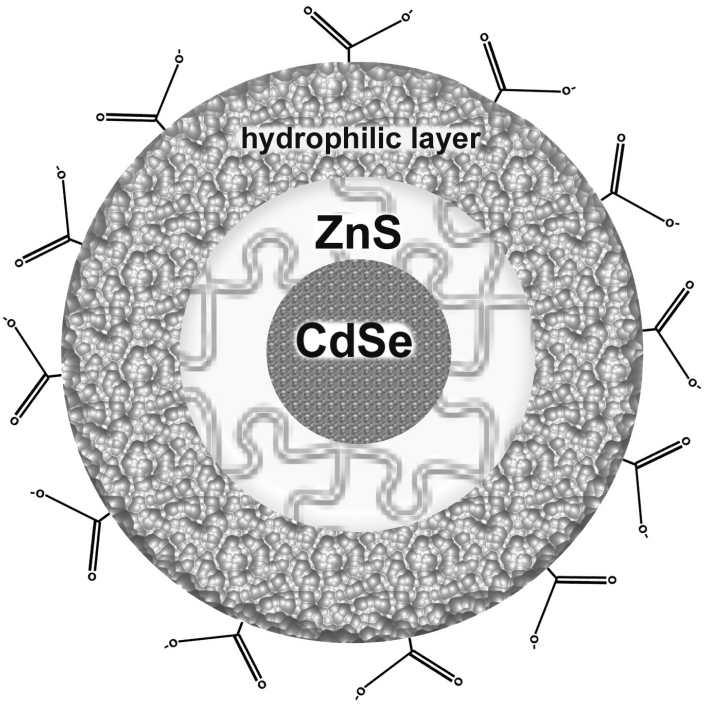

Figure 1 A diagram of the composition of a single CdSe/ZnS core/shell quantum dot nanocrystal with a hydrophilic layer that provides the COOH groups.

However, there are several concerns associated with using QDs in biological systems. The semiconductor material is not water-soluble, which means QDs must be coated with a hydrophilic layer prior to use in aqueous environments such as live cells[3]. This layer increases their size and modifies their properties. Secondly, their general optical and chemical properties are not yet fully characterized or understood. For example, although water-soluble QDs have been successfully used in live cells[2,4–6], their general compatibility with the cellular environment is not firmly established.

This paper describes observations relating to the reaction of living mammalian cells (rat cells) to the introduction of water-soluble quantum dots with different hydrophilic layers. Our results indicate that a deficient hydrophilic layer promotes aggregation of the QDs in solution. The aggregates not only have compromised optical properties, but also trigger a defensive reaction by the cells, limiting the applicability of QDs as a biological probe.

Background

The quantum dots used in this study were acquired from two different companies: Evident Technologies, Inc. (ET) and Quantum Dot Corporation (QDC). The peak emission wavelength of the ET QDs was 600 nm, and that of the QDC QDs was 605 nm. All QDs had a CdSe/ZnS core shell structure, but with different surface chemistries. Two types of QDs were purchased from ET; the first type functionalized with COOH groups (ET600COOH) and the second type with NH_2 groups (ET600NH_2). Only one type of QDs, functionalized with NH_2 groups, was purchased from QDC (QDC605NH_2).

The size and tendency to aggregate of these different QDs were characterized by fluorescence correlation spectroscopy (FCS) and time-lapse video microscopy (TLVM). FCS is a technique based on the analysis of fluorescence fluctuations[7,8]. We used FCS to estimate the size of QDs by measuring their diffusion coefficient.

Aggregates are collections of QDs tightly associated with each other mainly through the electrostatic interactions caused by an imperfect hydrophilic layer[2]. Such groupings are expected to behave as large, slow-moving fluorophores with altered fluorescence properties. Hence, they can be easily detected and characterized with FCS studies.

The FCS instrument uses a 543.5 nm helium-neon laser as the excitation light source. The laser beam is tightly focused through a high numerical aperture water immersion objective (60x magnification, 1.33 NA) onto the sample, which is located on a TE2000U Nikon inverted epi-fluorescence microscope (see Figure 2). The sample chambers are made using a glass slide and a coverslip separated by parafilm spacers and sealed with wax. The fluorescence emitted by molecules in the focal volume is collected by the same objective, passed through a dichroic mirror and an emission filter to remove the excitation light, focused through a pinhole to eliminate out-of-focus fluorescence, and detected by a sensitive photomultiplier tube with a time resolution of 60 ns.

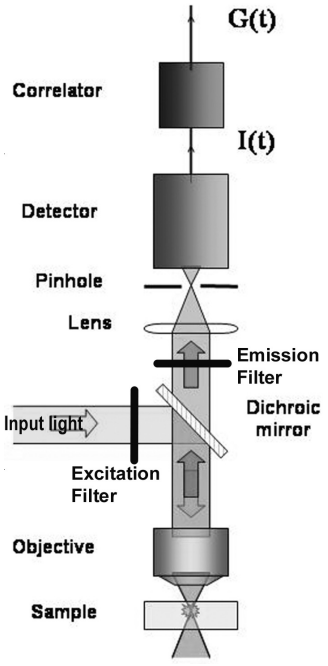

Figure 2 A schematic of the FCS setup used to measure the radius of different QDs.

In order to characterize the temporal fluctuations of the QDs, the signal is fed into a correlator card that computes its autocorrelation function (ACF) using an established algorithm that separates fluctuation events occurring with different characteristic times. Fluorescence fluctuations arise for different reasons, including the diffusion of fluorescent particles across the focal volume. Each kind of fluctuation is reflected in the ACF by a smooth decay rate. In the case of fluctuations due to diffusion, the corresponding decay time observed in the ACF is equal to the average residence time of a fluorescent particle in the focal volume.

Fitting the ACF with an appropriate model allows the extraction of several parameters: the diffusion constant, concentration and molecular brightness of the fluorescent particles. The QD data were fit assuming either that only one species was diffusing in solution (a one-component model) or that two different species were diffusing in solution (a two-component model).

For one fluorescent species diffusing in solution, the autocorrelation function is of the form

$$G(t) = \frac{1/N}{\left(1+4Dt/w_0^2\right)\sqrt{1+4Dt/S^2w_0^2}}\left(1+\frac{Te^{-t/\tau_T}}{1-T}\right), \quad (1)$$

where N is the average number of fluorescent molecules in the detection volume and D ($\mu m^2/s$) is their diffusion coefficient[8]. The second term uses exponential statistics to account for fast photophysical phenomena, such as blinking due to the existence of a non-fluorescent triplet state of the particles, or for rotation of particles. In the case of blinking, T is the average fraction of molecules found in the non-fluorescent state and τ_T (s) is the characteristic relaxation time associated with the blinking. Both S and w_0 (μm) are constant parameters describing the geometry of the detection volume.

In the case when two different fluorescent species diffuse in solution with respective diffusion coefficients D_1 and D_2 ($\mu m^2/s$), the autocorrelation function is

$$G(t) = \left(\frac{1/N_1}{\left(1+4D_1t/w_0^2\right)\sqrt{1+4D_1t/S^2w_0^2}} + \frac{1/N_2}{\left(1+4D_2t/w_0^2\right)\sqrt{1+4D_2t/S^2w_0^2}}\right)\left(1+\frac{Te^{-t/\tau_T}}{1-T}\right), \quad (2)$$

where N_1 and N_2 are effective parameters depending on both the concentration and the molecular brightness of the two different fluorophores.

The diffusion coefficients D, D_1 and D_2 in Equations (1) and (2) are used to calculate the hydrodynamic radius of the QDs. The hydrodynamic radius is an effective parameter defined as the radius of a sphere with the same diffusion coefficient as the particle in question. The hydrodynamic radius is generally larger than the physical radius of the QD due to the electrostatic attraction of water molecules to the hydrophilic layer of the QDs, which creates a water shell around the QDs. The hydrodynamic radius R of a molecule is calculated from its diffusion coefficient D using the Stokes-Einstein relationship,

$$D = \frac{k_B T}{6\pi\eta R}, \quad (3)$$

where k_B is the Boltzmann constant (J/K), T is the absolute temperature (K), and η is the viscosity of the solution.

Time-lapse video microscopy (TLVM) uses a fluorescence microscope in conjunction with an image acquisition system to determine the exact location and intensity of light from fluorophores in the field of view at different points in time[4,10,11]. Hence, TLVM can be used to track the motion of fluorophores through the field of view. TLVM was performed on the TE2000U Nikon inverted microscope setup described above, with an infrared-filtered Mercury arc lamp as the light source. Images were collected using a frame transfer camera (Ropers Scientific, MicroMax 512BFT) and accompanying WINView software, and were analyzed using ImageJ and Adobe Photoshop.

The QDs were introduced into the cells using pinocytic loading, a non-invasive method that relies on the natural ability of cells to ingest fluids using its cell membrane. Cells normally ingest fluids by pulling in a portion

of their cell membrane and pinching the ends to form a fluid-filled compartment called a vesicle. This process allows the cell to intake small soluble molecules along with the fluid.

In order to use this method to introduce the QDs into cells, mammalian Rat1 cells were plated on a coverslip-bottom chambered dish at about 25% confluency approximately 24 hours prior to the experiment. The cells were then incubated for 10 minutes at 37°C in a hypertonic solution containing the QDs.

This hypertonic solution has a high concentration of solutes relative to the cell interior; thus, it dehydrates the cells and accelerates their intake of material (including QDs) from the surrounding hypertonic solution into the membrane-bound vesicles. Next, the cells were placed in a hypotonic solution for 3 minutes. A hypotonic solution has a low concentration of solutes relative to the cell interior so it induces the cells to break these vesicles, releasing the QDs into the cell interior. After that, the cells were allowed to recover in a fresh culture medium – a solution that maintains conditions ideal for cell growth – for at least 7 minutes at 37°C.

We also fluorescently labelled lysosomes – structures used by the cell to degrade organic molecules – to check for the presence of QDs inside them. To label the lysosomes, the cells were further incubated in medium containing 60 nM (nanomoles/liter) of Lysotracker dye for 3 minutes at 37°C and washed with phosphate-buffered saline (PBS), a colourless solution used to maintain a constant pH of 7.4.

Imaging of live cells was performed by TLVM as described above. The cells were placed in PBS, as opposed to a cell growth medium, in order to reduce background fluorescence. The temperature in the sample was maintained at 37°C throughout the experiment by means of a stage and objective heater. A shutter system controlled the excitation light and reduced photodamage. The QDs were excited around 560 nm, and the emission of the QDs was detected around 600 nm using an appropriate filter set and the image acquisition system described above. Similarly, the Lysotracker dye was excited around 480 nm and the emission was detected around 535 nm using a second filter set.

Results

MEASUREMENT OF THE RADIUS OF THE QUANTUM DOTS

In order to characterize the size of the quantum dots used in this study, FCS data was collected for each of the three types of QDs described above. Some of the recorded autocorrelation functions are shown in Figure 3.

The data obtained for the QDs purchased from the Quantum Dot Corporation were successfully fit using a one-component diffusion model to within an error of approximately 1%. The average particle radius of 13.9 ± 0.1 nm extracted using this model is consistent with the manufacturer's prediction (see Table 1).

Quantum dot type	Radius of the first component (nm)	Radius of the second component (nm)	Brightness per molecule (photons/s)
QDC605NH_2 Unfiltered	13.9 ± 0.1	NA	62 ± 1
ET600NH_2 Filtered	19.8 ± 0.1	NA	16.0 ± 0.3
ET600NH_2 Unfiltered	Fixed at 19.8	160 ± 20	NA
ET600COOH Unfiltered	Fixed at 19.8	150 ± 40	NA

Table 1 A summary of the FCS data in solution for three types of quantum dots. Unfiltered QDC605NH_2 and filtered ET600NH_2 were fit with a one-component model, while unfiltered ET600NH_2 and unfiltered ET600COOH were fit with a two-component model.

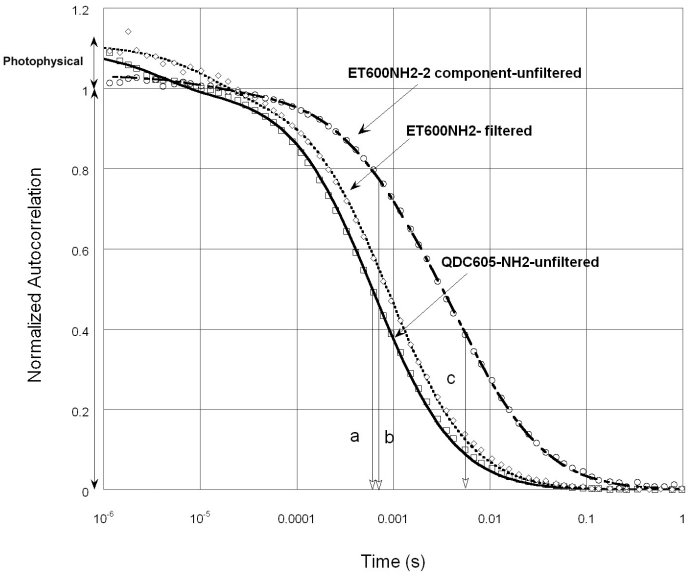

Figure 3 Autocorrelation functions obtained by FCS for different types of QDs (squares: QDC605NH_2, circles: ET600NH_2, diamonds: filtered ET600NH_2) and fit with Equations (1) or (2). The diffusion of the smaller single QDC605NH_2 quantum dots results in a short diffusion time (a). Two-component modeling of the unfiltered ET600NH_2 QDs gives the diffusion time of the single QDs (b) and that of the aggregates (c). A shift of the ACF decay towards larger time scales, indicating the presence of aggregates, is visible only in the unfiltered ET600NH_2 QDs. A second decay, due to an uncharacterized effect, is indicated by the double headed arrow labeled 'photophysical' at short times for the ACFs of the single QDs only.

In contrast, the data obtained for the Evident Technologies QDs could not be satisfactorily fit with a one-component model, as shown by a large discrepancy between the experimental autocorrelation function and the fit, which was interpreted as a signature of the presence of aggregates. Using a two-component model yielded better results, determining the aggregate's radius with an error of less than 30%. This two-component model had a fast diffusing component accounting for the presence of single QDs, and a slow diffusing component accounting for the presence of aggregates.

When subjected to an additional 10 minute, 21 000 g centrifugation step (ultra-filtration), the ET QDs exhibited a narrow size distribution with an average radius of 19.8 ± 0.1 nm, in agreement with the manufacturer's specifications (see Table 1). For the fit of the unfiltered ET QD samples, the first species (corresponding to single QDs) was assigned a fixed radius of 19.8 nm by applying the results of the filtered QDs. The diffusion time of the first species was determined within an error of 1% using filtered QDs made of the same material from the same manufacturer. With only one parameter to determine, the radius of the aggregates was estimated at 150 nm (see Table 1). Since it is not expected that aggregates all have exactly the same size, the two-component model was used only as an approximation of the real system.

In addition, it was found that the QDC605NH_2 were about 4 times brighter than the ET600NH_2 (see Table 1).

OBSERVATION OF THE QUANTUM DOTS BLINKING

In order to test the capacity of our fluorescence imaging system to detect single fluorophores, QDs were immobilized in a 5% polyacrylamide gel and imaged using TLVM as described above. A characteristic image is shown in Figure 4a. Some of the bright spots observed in these images had an intensity that greatly fluctuated over time, sometimes reaching an intensity that could not be distinguished from the background intensity (see Figure

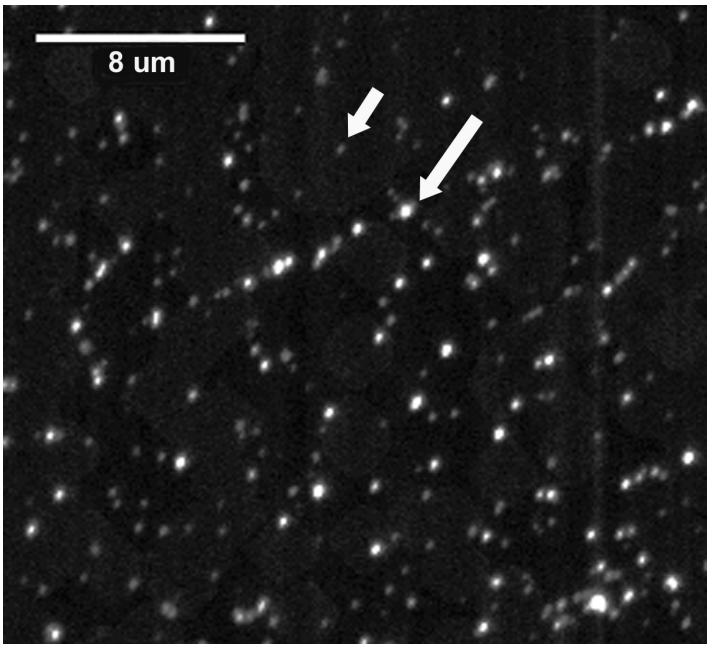

Figure 4a TLVM image of unfiltered ET600COOH QDs embedded in a 5% polyacrylamide gel. The long arrow points to an aggregate and the short arrow points to a single QD.

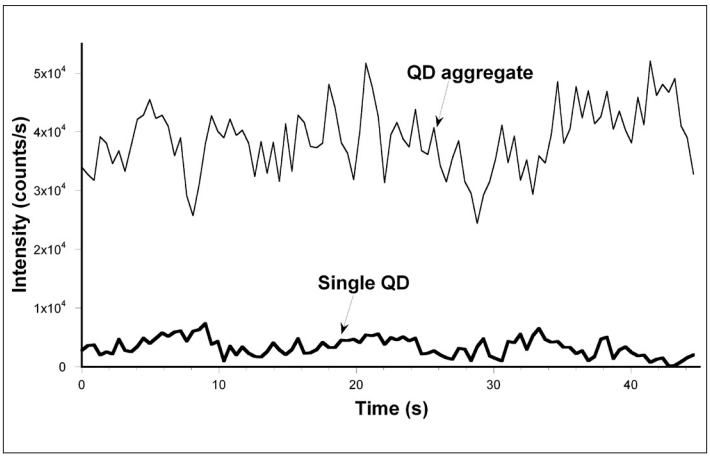

Figure 4b Fluorescence intensity as a function of time for a particle identified as a single QD (thick black line) and a particle identified as an aggregate (thin grey line). These QDs were embedded in 5% polyacrylamide gel and imaged using TLVM with a time resolution of 100 ms. In each case, the intensity was calculated by adding the intensity value of nine pixels identified as representing the image of the particle. A background value was subtracted from both intensities.

QD type	Directed motion?	Diffusion coefficient ($\mu m^2/s$)	Velocity ($\mu m/s$)	Brightness (counts/s)
QDC605NH_2 Filtered	No	0.71 ± 0.02	NA	1800 ± 40
ET600NH_2 Filtered	No	0.19 ± 0.01	NA	1200 ± 30
ET600COOH Unfiltered	Yes	NA	0.18–0.26 ± 0.02	3700 ± 60

Table 2 A summary of TLVM data for filtered and unfiltered QDs purchased from QDC and ET, and loaded into Rat1 cells.

4b). This on-and-off fluorescence behaviour, or blinking, is characteristic of single QDs[9,13].

The intensity of these single QDs did not disappear completely due to the exposure time (100 ms) of the image acquisition system being slightly longer than ideal. However, our ability to distinguish single QDs from aggregate QDs demonstrates the sensitivity of the fluorescence imaging system. Aggregates had a higher absolute intensity, but with lower relative fluctuations in amplitude. Blinking was observed for all three types of QDs studied.

In the FCS curves corresponding to the diffusion of single QDs (QDC605NH_2 and filtered ET600NH_2), a second decay was observed at microsecond time-scales (see double headed arrow labeled 'photophysical' in Figure 3). This decay was consistently accounted for by the second term in Equations (1) and (2), with an error of less than 7%. This shows that there was a fast photophysical effect, such as blinking due to the non-fluorescent triplet state or rotation, taking place for single QDs that follows exponential statistics as described in the second term of Equations (1) and (2). However, this photophysical effect is different from the blinking effect of single QDs observed by TLVM at longer time-scales, which is known to have power law statistics[12] (see Figure 4b). More work is needed to characterize both of these types of blinking effects.

CHARACTERIZATION OF THE LOCALIZATION AND MOTION OF QUANTUM DOTS IN LIVE CELLS

In order to study the behaviour of QDs in live cells, each of the three types of dots were introduced into Rat1 cells (mammalian fibroblasts derived from rats) using the pinocytic loading method described above, and imaged after two hours. Two very different types of behaviour were observed. Aggregated QDs (unfiltered ET600COOH and unfiltered ET600NH_2) localized into punctuated structures, and did not appear to blink.

We suspected that these structures might be lysosomes – acidic organelles used by cells to degrade organic molecules. In order to test this hypothesis, the cells were imaged after incubation with a Lysotracker dye which stains acidic structures in the cell, particularly lysosomes. Images were taken with different filter sets in order to image either the QDs or the lysosomes for the same cell. The cells recognized both unfiltered ET600COOH and unfiltered ET600NH_2 aggregates, and processed them in similar ways. This indicates that QD aggregates are recognized in cells regardless of their surface composition. Figure 5 illustrates the result of such an experiment, showing that aggregated QDs do indeed colocalize with lysosomes. In contrast, those QDs that behaved as single QDs in solution (QDC605NH_2 and filtered ET600NH_2) were randomly distributed throughout the cell cytoplasm, did not colocalize with the lysosomes and were blinking (data not shown).

This cellular response to single QDs and aggregates was confirmed by tracking QD motion inside cells. Tracking of QDs was performed by following a QD over time, alternating between the two filter sets described above. Tracking of the unfiltered ET600COOH confirmed that they might be enclosed in lysosomes, as their motion was consistent with the directed motion expected for these organelles. The image sequence in Figure 6 follows the motion of an ET600COOH aggregate. This motion is directed (i.e., it takes place along a linear path) and saltatory (i.e., dwell times are observed where the particles exhibit no visible motion). Given the time elapsed and average displacement between two frames, the average velocity of these QD aggregates was between 0.18 and 0.26 $\mu m/s$ (see Table 2). These velocities are consistent with motor protein transport of cargos along microtubules[10,11].

In contrast, tracking of QDC605NH_2 (see Figure 7) and filtered ET600NH_2 (data not included) showed QDs freely diffusing through the cytoplasm, with a trajectory resembling that of Brownian motion. The diffusion coefficients D of these two types of QDs was determined from their average mean square displacement $\langle r^2 \rangle$ between two video frames,

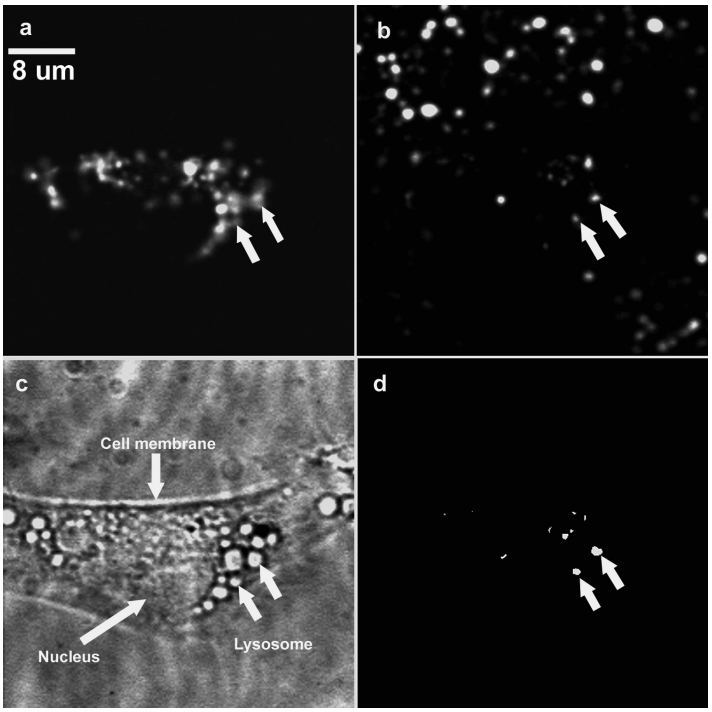

Figure 5 Different images of the same Rat1 fibroblast cell loaded with unfiltered ET600COOH QDs and stained with a Lysotracker dye. (a) TLVM image showing the position of the lysosomes. (b) TLVM image showing the position of the QDs (note the presence of QDs absorbed on the coverslip outside of the cell). (c) Light microscopy transmission image. (d) TLVM colocalization image showing the overlap of the fluorescence signal coming from the lysosomes and that coming from the QDs. The arrows indicate the position of two lysosomes containing QD aggregates.

$$D = \frac{\langle r^2 \rangle}{4\Delta t}, \tag{4}$$

where r (μm) is the displacement and Δt (s) is the time between frames. Image analysis also indicated that QDC605NH_2 was 1.5 times brighter and diffused 3.7 times faster than ET600NH_2 (see Table 2).

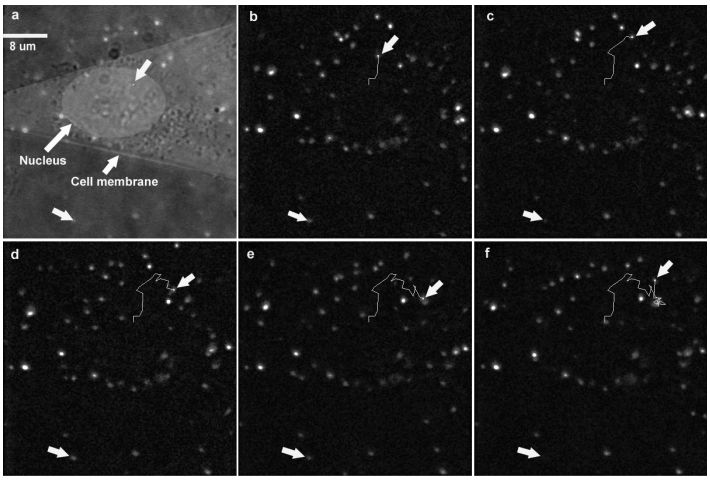

Figure 7 Image (a) shows the overlay of a light microscopy transmission image of a Rat1 fibroblast cell with the TLVM image of QDC605NH_2 QDs. Each subsequent image tracks the diffusive motion of a single QD in the cell. The bottom arrow in the image sequence shows the blinking of a single QD attached to the coverslip.

Discussion

Our comparison of three different types of quantum dots in solution using fluorescence correlation spectroscopy indicates that the surface coating used by Evident Technologies Inc. is more likely to promote aggregation than the coating used by Quantum Dot Corporation, and result in QDs which are significantly dimmer and 30% larger than the Quantum Dot Corporation's QDs.

Consistent with this last observation, we also found that the diffusion coefficient in cells of the QDC QDs was smaller than that of the ET QDs. However, based on the Stokes-Einstein relationship, the diffusion coefficient should be proportional to the radius of the diffusing particle, so that we would expect a 30% difference instead of the observed 73% difference. This discrepancy could be explained either by the binding of QDs to cellular proteins, the aggregation of the ET QDs when placed in the cellular medium, or by the complexity of the cellular environment that invalidate the Stokes-Einstein relationship.

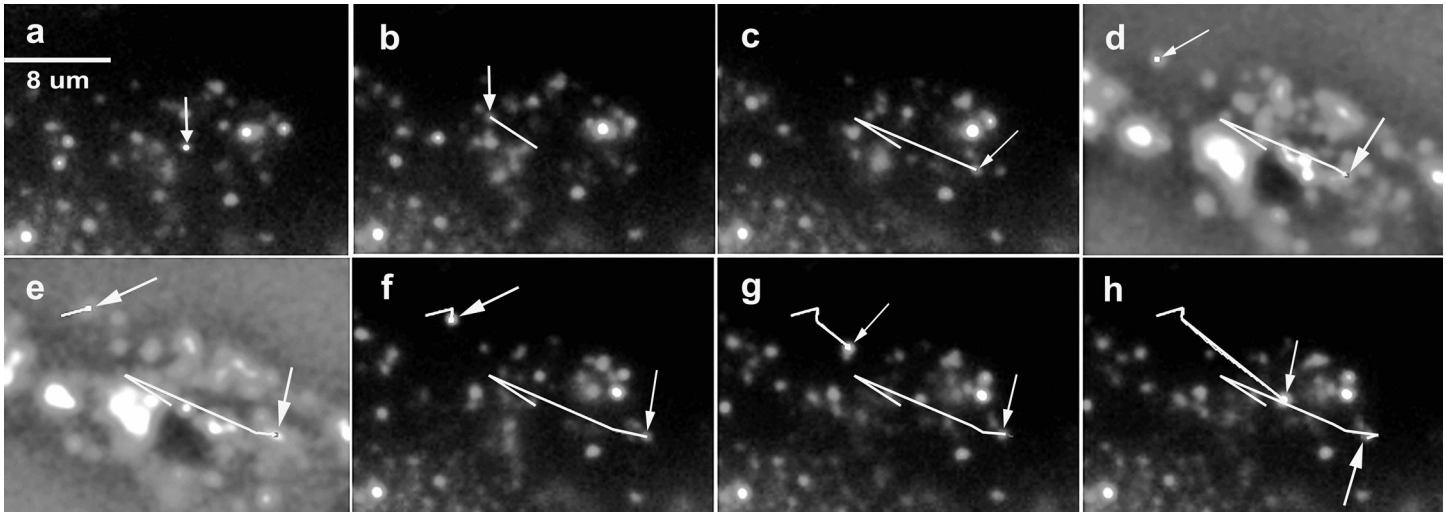

Figure 6 Sequence of TLVM images showing the directed cellular motion (presumably along a microtubule) of two ET600COOH aggregates within lysosomes. The positions of the aggregates are indicated by arrows and their paths by a continuous line. Images (a), (b), (c), (f), (g) and (h) show the fluorescence of the QDs and images (d) and (e) show the fluorescence of the lysosomes. This chronological sequence of images was captured by alternating between two filter sets for imaging QDs and lysosomes.

Our time-lapse video microscopy experiments showed that a tendency to aggregate can have profound consequences for the reaction of cells to QDs irrespective of their surface composition. The Rat1 cells used in this study recognized QD aggregates and packaged them into lysosomes for destruction. However, remarkably, these cells failed to recognize single QDs as foreign objects. These results further demonstrate that single QDs are useful biological probes as long as they have the appropriate surface chemistry to inhibit aggregation and maintain their optical properties.

Conclusion

Our fluorescence correlation spectroscopy and time-lapse video microscopy experiments show that deficient surface coating promotes aggregation of the QDs in an aqueous environment in vitro. More importantly, colocalization studies and tracking of QDs in living cells indicate that cells recognize aggregates of QDs, but not individual QDs, as foreign bodies. The reaction of cells to QDs is hence immensely dependent upon the surface chemistry of the QDs. An inappropriate surface coating introduces undesirable effects such as aggregation and reduced brightness per molecule and compromises the potential of the QDs to be used as fluorescent probes to study sub-cellular dynamics.

References

[1]J.K. Jaiswal and S.M. Simon. "Potentials and pitfalls of fluorescent quantum dots for biological imaging." *Trends in Cell Biology.* (2004) **14**(9), pp. 497–504.

[2]K. Hanaki, *et al*. "Semiconductor quantum dot/albumin complex is a long-life and highly photostable endosome marker." *Biochemical and Biophysical Research Communities*. (2003) **302**(3), pp. 496–501.

[3]W.C. Chan and S. Nie. "Quantum dot bioconjugates for ultrasensitive nonisotopic detection." *Science*. (1998) **281**(5385), pp. 2016–2018.

[4]M. Dahan, *et al.* "Diffusion dynamics of glycine receptors revealed by single-quantum dot tracking." *Science*. (2003) **302**(5644), pp. 442–445.

[5]J.K. Jaiswal, *et al.* "Long-term multiple color imaging of live cells using quantum dot bioconjugates." *Nature Biotechnology*. (2003) **21**(1), pp. 47–51.

[6]D.S. Lidke, *et al.* "Quantum dot ligands provide new insights into erbB/HER receptor-mediated signal transduction." *Nature Biotechnology*. (2004) **22**(2), pp. 198–203.

[7]D. Magde, E. Elson, and W.W. Webb. "Thermodynamic fluctuations in a reacting system-measurement by fluorescence correlation spectroscopy." *Physical Review Letters* (1972) **29**(11), pp. 705–708.

[8]M.A. Medina and P. Schwille. "Fluorescence correlation spectroscopy for the detection and study of single molecules in biology." *Bioessays*. (2002) **24**(8), pp. 758–764.

[9]S. Hohng and T. Ha. "Near-complete suppression of quantum dot blinking in ambient conditions." *Journal of American Chemical Society.* (2004) **126**(5), pp. 1324–1325.

[10]E. Vignal, *et al.* "Kinectin is a key effector of RhoG microtubule-dependent cellular activity." *Molecular and Cellular Biology.* (2001) **21**(23), pp. 8022–8034.

[11]B. Herman and D.F. Albertini. "A time-lapse video image intensification analysis of cytoplasmic organelle movements during endosome translocation." *The Journal of Cell Biology.* (1984) **98**(2), pp. 565–576.

[12]M. Kuno, *et al.* "Nonexponential 'blinking' kinetics of single CdSe quantum dots: A universal power law behaviour." *Journal of Chemical Physics.* (2000) **112**(7), pp. 3117–3120.

[13]M. Kuno, *et al.* "'On'/'Off' fluorescence intermittency of single semiconductor quantum dots." *Journal of Chemical Physics.* (2001) **115**(2), pp. 1028–1040.

Saint Mary's University
Halifax, Nova Scotia, Canada

Department of Astronomy and Physics

Ph.D. and M.Sc. Programs in Astronomy

- Eleven faculty members in the department, eight of whom have expertise in theoretical astrophysics and observational astronomy
- **Research areas:** stellar evolution, stellar seismology, stellar atmospheres, nuclear astrophysics, MHD astrophysics, extragalactic astronomy, galactic structure, star clusters, interstellar medium, variable stars, star formation, planet formation, and planetary dynamics
- Extensive computational facilities, including those of the Institute for Computational Astrophysics (ICA) and ACEnet
- Full financial support is provided to all full-time students

For more information contact:
Graduate Coordinator
Department of Astronomy and Physics
Saint Mary's University
Halifax NS B3H 3C3

Phone: (902) 420-5828
E-mail: graduate@ap.smu.ca
URL: www.ap.smu.ca